Growth Morphology of Vicinal Hillocks on the {101} Face of KH_2PO_4: From Step-Flow to Layer-by-Layer Growth

J. J. De Yoreo, T. A. Land, and B. Dair
Lawrence Livermore National Laboratory, Livermore, California 94550
(Received 18 March 1994)

The growth morphologies of vicinal hillocks on KH_2PO_4 {101} surfaces have been investigated using atomic force microscopy. Growth occurs on monomolecular steps both by step-flow and through layer-by-layer growth on both dislocation induced steps and 2D nuclei. Dislocation induced hillocks exhibit hollow cores. The circular cross sections of these cores are consistent with an isotropic step edge energy and the core radii are in good agreement with theoretical predictions. From the interisland spacing we estimate the surface diffusion length to be 200 to 300 nm at 300 K.

PACS numbers: 61.50.Cj, 61.16.Ch, 61.72.Lk, 68.35.Bs

In recent years, the nanometer-scale morphology of crystalline surfaces has received considerable attention, in part because of its control on materials properties and performance. Most studies have considered the growth of surfaces by molecular beam epitaxy or chemical vapor deposition where the system is generally far from equilibrium both in terms of the flux of impinging molecules and the chemical potential. It has been shown both theoretically [1,2] and experimentally [2] that, in this regime, growth progresses either by step flow at preexisting steps on vicinal surfaces or through layer-by-layer and multilayer growth on nucleating islands. For example, during the growth of Si at typical deposition conditions, the critical nucleus consists of only a single atom, as shown in scanning tunneling microscopy studies [3]. Few studies [4–6] have given attention to the nanometer-scale morphology of single crystal surfaces grown at low-to-moderate supersaturation, where stable islands consist of tens of molecules and the classic dislocation controlled mode of growth first described by Burton, Cabrera, and Frank (BCF) [7] should be applicable, despite the fact that most bulk single crystals are grown in this regime. Only one such investigation [8] has addressed the question of whether surface diffusion is an important mechanism during the growth of crystals from solution. Gratz, Hillner, and Hansma [8], using atomic force microscopy (AFM) to observe, *in situ*, the growth of calcite, found that growth occurred only on screw dislocations and did not observe 2D nucleation and growth even at relative supersaturations in excess of 300%. They also concluded that surface diffusion lengths were much less than the step spacings and that growth occurred through step flow by incorporation of monomers at step edges directly from the solution.

The purpose of this paper is to investigate the advance of single crystal surfaces from solution to low to moderate supersaturations. We report AFM results on the growth morphology of KH_2PO_4 (KDP), a system in which the fundamental growth parameters, α, the step edge energy, and β, the kinetic coefficient relating the step velocity to the supersaturation, are known, allowing us to make a direct comparison between theory and experiment. We show that even on vicinal hillocks where the Burgers vector exceeds one unit step the {101} surface advances on monomolecular steps. We calculate local supersaturations from the hillock slopes and measured Burgers vectors and compare our observations to the predictions of BCF-type theories. For Burgers vectors of more than one unit step, the hillocks are observed to contain hollow cores. The sizes of these cores compare well with theoretical predictions and the shape demonstrates for the first time that the step edge energy is isotropic. We show that, at moderate supersaturations (~10%), the growth of KDP {101} surfaces occurs both on dislocation induced steps and on islands formed by 2D nucleation. Furthermore, on the terraces of the vicinal hillocks formed by 2D nucleation, island growth competes with step flow when the interisland spacing is comparable to the terrace width. The distribution of islands shows that surface diffusion plays an important role in determining the rate of crystallization of KDP-like crystals.

The results presented here were obtained on samples prepared *ex situ*. While we have obtained AFM images of KDP during *in situ* growth, typical growth rates make it impossible to access a wide range of supersaturation. For example, at a relative supersaturation of only 2%, the surface advances by about 100 molecular layers per second. Samples grown in unstirred solutions at 300 K were drawn from solution through a hexane bath to preserve the surface. The samples were then transferred to the AFM for analysis.

Vicinal hillocks on the {101} face of KDP exhibit an asymmetric triangular anisotropy related to the crystal structure [9]. An AFM image of one such hillock is shown in Fig. 1(a) and illustrates this anisotropy. In the discussion that follows, the steepest slope is referred to as sector 1 and the shallowest as sector 3. Figure 1(b) shows a higher resolution image of steps on the side of the hillock. The height of these steps is 5 Å, which, within experimental error, is equal to half the unit cell parameter

0031-9007/94/73(6)/838(4)$06.00

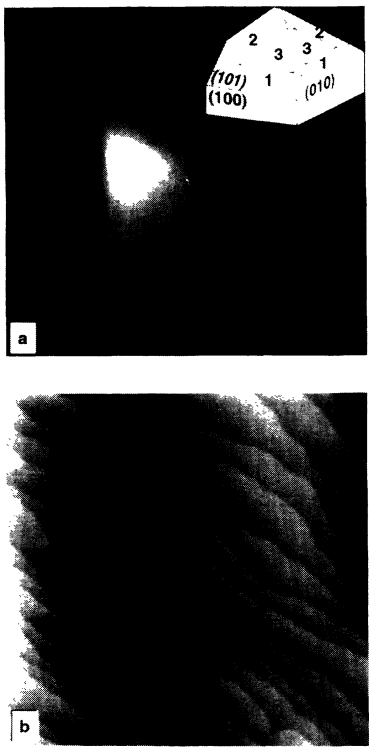

FIG. 1. (a) 35 × 35 μm AFM image of a vicinal hillock on the {101} face of KDP. (b) Individual steps on one 3 × 3 μm sector of the hillock. Each step is 5 Å in height. Inset to (a) shows schematic of growth hillock geometry on KDP.

of 10.2 Å in the ⟨101⟩ direction. This corresponds to the distance between K planes and is one monomolecular layer in thickness.

In their classic work on the growth of crystals, BCF [7] showed that, at low supersaturations, the advance of a crystal surface should occur on growth spirals consisting of monomolecular steps generated by screw dislocations. Within the BCF formalism, the relationship between the slopes p_i of a hillock with triangular anisotropy formed by a single dislocation and the critical radius r_c (the radius of the smallest stable island) is given by [9]

$$p_i = \frac{mh}{3.67\sqrt{3} r_c b_i \sum_{j=1}^{3} b_j^{-1}}, \quad (1)$$

where m is the net number of unit steps in the component of the Burgers vector perpendicular to the surface, h is the unit step height, and $b_1{:}b_2{:}b_3 = 1/p_1{:}1/p_2{:}1/p_3$ and depends only on the anisotropy in the kinetic coefficient β. The critical radius is related to the supersaturation σ by [7]

$$r_c = \omega\alpha/kT\sigma, \quad (2)$$

where ω is the specific molecular volume, 9.68×10^{-23} cm^3 for KDP, α is the step edge energy per unit step height, k is Boltzmann's constant, and T is the temperature. By combining AFM measurements of m and the p_i with $\alpha = 20$ mJ/m^2 obtained in previous studies [10], r_c and σ can be determined.

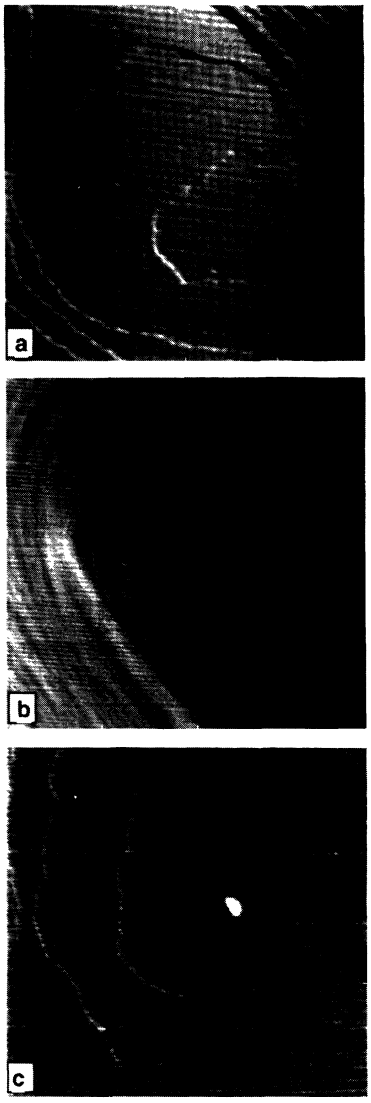

FIG. 2. AFM images of vicinal hillocks on KDP {101} with Burgers vectors of (a) one, (b) two, and (c) three unit steps. Each step is 5 Å in height. Derivative images are given to accentuate the steps. Image sizes are (a) 4.0 × 4.0 μm, (b) 1.8 × 1.8 μm, and (c) 1.5 × 1.5 μm.

Figures 2(a), 2(b), and 2(c) show the topmost portion of three growth spirals on the {101} face of KDP for which $m = 1$, 2, and 3, respectively. In each case, $p_1{:}p_2{:}p_3 = 4.1{:}2.1{:}1$. (The p_i were measured below the first few turns of the spiral, where the hillock steepens and the slope becomes constant.) Using Eqs. (1) and (2), we calculate supersaturations of (5.4 ± 0.1)%, (4.3 ± 0.2)%, and (4.0 ± 0.1)% for the three hillocks. The corresponding values of r_c determined from Eq. (2) are 87, 109, and 117 Å, respectively.

All observed spirals were composed of elementary steps regardless of the Burgers vector. While far from the hillock tops these steps were observed to have approximately equal spacing [see Fig. 1(b)], near the tops of spirals for which $m > 1$ the steps emerged

from the dislocations in groups of order m. This step homogenization with time is evidence for the existence of a Schwoebel barrier [11,12] as well as the importance of surface diffusion and shows that the diffusion length of adsorbed monomer is comparable to the terrace width. Steps above broad terraces can draw monomer from larger areas than those above narrow terraces and therefore they move more rapidly, eventually equalizing the interstep distances. The importance of surface diffusion is further discussed below.

Through thermodynamic considerations of the effects of stress, Frank [13] concluded that, for sufficiently large Burgers vectors, a growth spiral should contain a hollow core whose radius is given by

$$r_0 = \mu b^2/8\pi^2 K\alpha\,, \qquad (3)$$

where μ is the rigidity modulus, b is the Burgers vector, and K is a geometric parameter equal to 1 for screw dislocations perpendicular to the crystal face. As Fig. 2 shows, for $m > 1$, the growth hillocks contain hollow cores. Taking $\mu = 0.5(C_{11} - C_{12})$ [14], and using the values C_{11} and C_{12} from Ref. [15], for the hillock of Fig. 2(b) ($m = 2$), we obtain for r_0 a value of 25 nm. The measured core radius in Fig. 2(b) is ~14 nm, which is about half of r_0.

The derivation of (3) assumed that continuum elasticity theory was valid at the dislocation core. It was modified by Van der Hoek, Van der Eerden, and Bennema [16] who incorporated a strain energy function to account for the deviation from continuum theory at the core. The predicted hollow core radius r_{hc} is less than r_0 for all $\sigma > 0$. Taking $r_c = 109$ Å as calculated above and using the analysis of Ref. [16], we obtain $r_{hc} = 0.50r_0$ or 13 nm, in excellent agreement with the measured radius of 14 nm. This result demonstrates for the first time that the inclusion of inelastic effects is required to account for the measured core radius.

For the hillock of Fig. 2(c) ($m = 3$), the analysis described above predicts values for r_0 and r_{hc} of 56 and 22 nm, respectively. The radius of the core in Fig. 2(c) is considerably less than 50 nm. (We can only determine with certainty the upper bound because the shape of the tip begins to influence our measurement when the slope of the hole exceeds that of the tip.) This again shows that the inclusion of inelastic effects is required to correctly predict the size of the hollow cores. For the hillock of Fig. 2(a) ($m = 1$), no hollow core is observed. However, the calculated values of r_0 and r_{hc} are 6 and 4 nm, respectively, which are below the lateral resolution of the measurement.

All hollow cores that we observed are circular in cross section. This demonstrates that the free energy of the step riser is isotropic and that the anisotropy in the hillock geometry is due not to the energetics of the monomer-step interactions, but to kinetic constraints on adsorption and diffusion (i.e., anisotropy in the kinetic coefficient β) as was assumed in the derivation of Eq. (1) [9]. This result is in contrast to that of Gratz, Hillner, and Hansma [8] who observed triangular dislocation cores in calcite.

Growth on the {101} faces of KDP is not confined to growth spirals. Figure 3(a) shows an AFM image of one of a number of hillocks that consisted of flat-lying, single-layer islands. As is clear from Fig. 3(b), there is no evidence for a screw dislocation at the top of such hillocks indicating that these islands have formed through 2D nucleation. 2D nucleation has also occurred on the interstep terraces of these hillocks. Figure 4 shows the common occurrence of islands near the boundary between sectors 2 and 3 of the hillock in Fig. 3(a). (In contrast, such islands were never observed on dislocation induced hillocks.) While most of the steps have approximately equal spacings, near the center of the image one of the steps has stopped advancing and is being overgrown by the upper step. As a result, the lower terrace has broadened and is covered by islands of one to three layers thickness. The other terraces contain smaller, single step-height islands whose average spacing is 270 nm. The terraces themselves have average widths of 390 nm on sector 2 and 840 nm on sector 3. In comparison, the terraces of even the shallowest dislocation induced hillock ($m = 1$) are only about one third as wide. No islands are observed on sector 1 for which the average terrace width is only 150 nm. Thus this hillock exhibits the transition from step-flow to layer-by-layer growth. When the average terrace width is greater than the island separation, growth proceeds layer by layer on nucleating islands. But when the converse is true, growth occurs by step flow [1,2].

The average island spacing is controlled both by the degree of supersaturation *and* the surface diffusion length x_s. Because the supersaturation is the same on all sectors of the hillock, the presence or absence of islands must depend on the size of the average terrace width relative to x_s. We conclude that x_s is on the order of 200 to 300 nm or 400 to 600 lattice sites. On terraces which are narrower than this, the steps act as sinks and no island formation takes place. On wider terraces, monomer can be incorporated into stable islands before it reaches a step. As a consequence of this process, the terraces of sectors 2 and 3 are covered at a rate which is more rapid than that for pure step flow, and the ratio of the slopes is anomalous. For the hillock of Fig. 3(a), p_1:p_2:p_3 = 5.6:2.2:1.0. Vekilov, Kuznetsov, and Chernov [9] concluded that surface diffusion is an important mechanism in determining the rate of advance of steps on KDP-like crystals and that the hillock anisotropy is due to differences in jump distances for diffusion on the three sectors, although little is known about the mechanism of diffusion or the diffusing species. Our results support the conclusion of Vekilov, Kuznetsov, and Chernov [9] and are in stark contrast to the conclusions of Gratz, Hillner, and Hansma [8] with respect to surface diffusion during the growth of calcite.

Within the BCF formalism and its later modifications, growth by 2D nucleation at low supersaturations is unlikely because of the large activation energy for formation of a nucleus whose radius exceeds that of the critical nu-

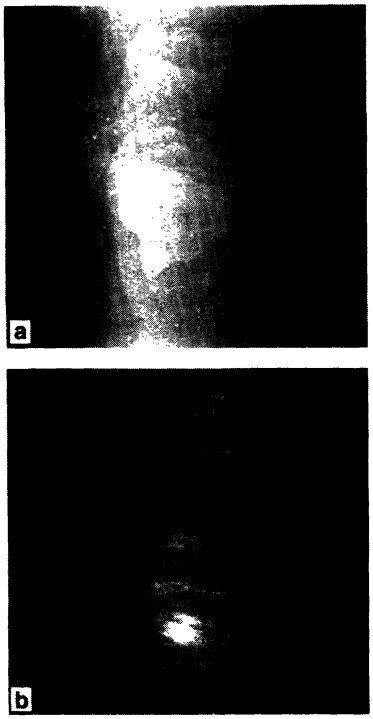

FIG. 3. (a) 5.4 × 5.4 μm AFM image of typical hillock on KDP {101} at which no dislocations are observed. (b) Higher resolution 715 × 715 nm image of one such hillock showing the topmost island for which the radius is 42 nm.

cleus. However, as the supersaturation increases, r_c decreases and the growth rate of 2D nuclei increases until it equals that for growth on screw dislocations, provided the ratio of the step edge energy α to the thermal energy kT is sufficiently small [17]. Using the expression [17]

$$R = \left(\frac{1+\sigma}{\sigma}\right)^{1/3} x_s^{4/3}\left[1 - \frac{1}{3}\left(\frac{19\omega\alpha}{2hkT\sigma x_s}\right)^{2/3}\right]^{-1} \times \exp\left[-\frac{\pi(\omega\alpha/hkT)^2}{3\sigma}\right], \quad (4)$$

the ratio of the rates of 2D to dislocation induced growth, R, can be estimated from the values of σ and α/kT, on which it is strongly dependent, and the diffusion length x_s, on which it is weakly dependent. Taking $x_s \sim 500$ lattice sites [9] we find that at $\sigma \sim 5\%$ $R \sim 10^{-3}$ while at $\sigma \sim 10\%$ this ratio is ~ 1. Thus, while at supersaturations below 5% growth is dominated by a dislocation mechanism, at supersaturations in excess of 5% growth on 2D nuclei begins to compete. At these supersaturations, growth of new islands and growth at existing step edges occur simultaneously and, as is seen in Fig. 4, if the growth of a step becomes impeded, 2D nuclei will readily cover the adjacent terrace.

We gratefully acknowledge Wigbert Siekhaus and Joe Lee for their assistance. This work was performed under the auspices of the U.S. Department of Energy by Lawrence Livermore National Laboratory under Contract No. W-7405-Eng-48.

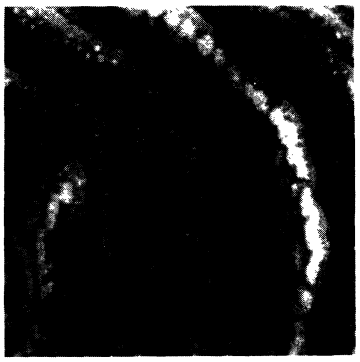

FIG. 4. 6.3 × 6.3 μm area near boundary between sectors 2 and 3 of hillock in Fig. 3(a). Note the presence of islands on all terraces.

[1] J. Tersoff, A. W. Denier van der Gon, and R. M. Tromp, Phys. Rev. Lett. **72**, 266 (1994).
[2] M. D. Johnson, C. Orme, A. W. Hunt, D. Graff, J. Sudijono, L. M. Sander, and B. G. Orr, Phys. Rev. Lett. **72**, 116 (1994).
[3] Y. W. Mo, J. Kleiner, M. B. Webb, and M. G. Lagally, Phys. Rev. Lett. **66**, 1998 (1991).
[4] A. J. Gratz, S. Manne, and P. K. Hansma, Science **251**, 1343 (1991).
[5] D. G. Schlom, D. Anselmetti, J. G. Bednorz, R. F. Broom, A. Catana, T. Frey, Ch. Gerber, H.-J. Güntherodt, H. P. Lang, and J. Mannhart, Z. Phys. B **86**, 163 (1992).
[6] S. D. Durbin and W. E. Carlson, J. Cryst. Growth **122**, 71 (1992).
[7] W. K. Burton, N. Cabrera, and F. C. Frank, Philos. Trans. R. Soc. London A **243**, 299 (1951).
[8] A. J. Gratz, P. E. Hillner, and P. K. Hansma, Geochem. Cosmochim. Acta **57**, 491 (1993).
[9] P. G. Vekilov, Yu. G. Kuznetsov, and A. A. Chernov, J. Cryst. Growth **121**, 44 (1992); **121**, 643 (1992).
[10] L. N. Rashkovich, A. A. Mkrtchyan, and A. A. Chernov, Sov. Phys. Crystallogr. **30**, 219 (1985).
[11] R. L. Schwoebel and E. J. Shipsey, J. Appl. Phys. **37**, 3682 (1966).
[12] R. Kunkel, B. Poelsema, L. K. Verheij, and G. Comsa, Phys. Rev. Lett. **65**, 733 (1990).
[13] F. C. Frank, Acta Crystallogr. **4**, 497 (1951).
[14] J. F. Nye, *Physical Properties of Crystals* (Oxford Univ. Press, New York, 1985), Chap. 13.
[15] *Landolt-Bornstein Tables of Numerical Data and Functional Relationships in Science and Technology*, edited by K.-H. Hellwege and A. M. Hellwege (Springer, New York, 1979), Group III, Vol. 11.
[16] B. Van der Hoek, J. P. Van der Eerden, and P. Bennema, J. Cryst. Growth **56**, 621 (1982). In the analysis, 3.48×10^8 J m^{-3} is used for enthalpy of melting of KDP.
[17] B. Lewis, in *Crystal Growth*, edited by B. R. Pamplin (Pergamon Press, Great Britain, 1980), Vol. 16, Chap. 2, p. 23.

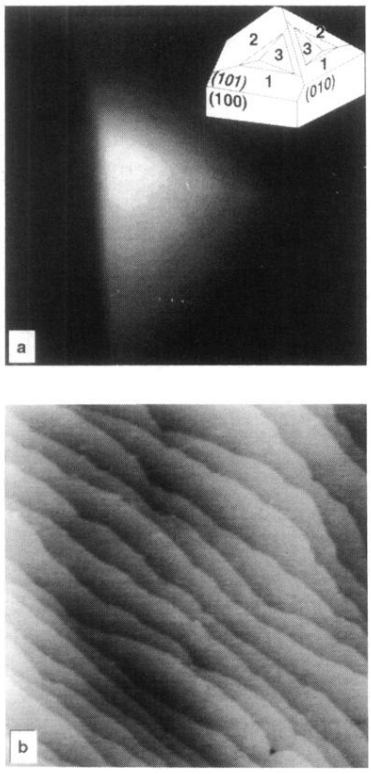

FIG. 1. (a) 35 × 35 μm AFM image of a vicinal hillock on the {101} face of KDP. (b) Individual steps on one 3 × 3 μm sector of the hillock. Each step is 5 Å in height. Inset to (a) shows schematic of growth hillock geometry on KDP.

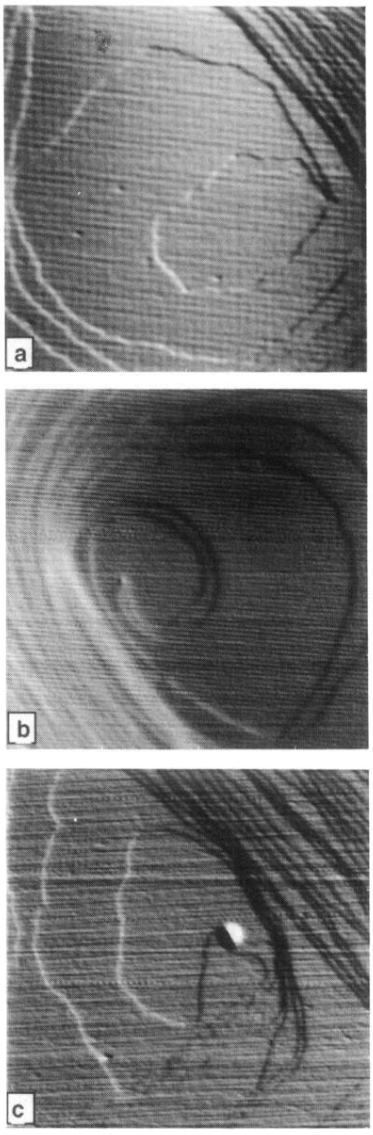

FIG. 2. AFM images of vicinal hillocks on KDP {101} with Burgers vectors of (a) one, (b) two, and (c) three unit steps. Each step is 5 Å in height. Derivative images are given to accentuate the steps. Image sizes are (a) 4.0×4.0 μm, (b) 1.8×1.8 μm, and (c) 1.5×1.5 μm.

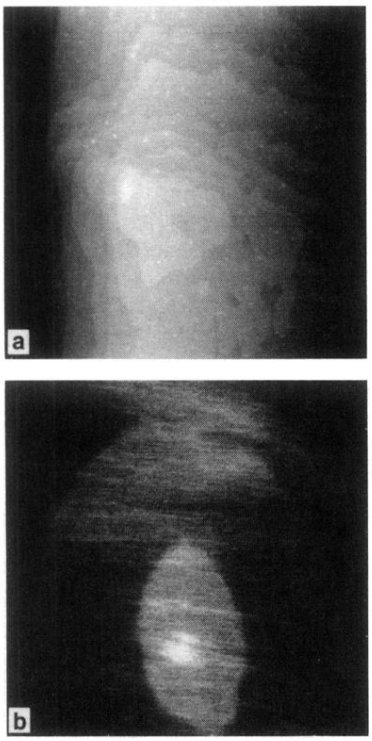

FIG. 3. (a) 5.4 × 5.4 μm AFM image of typical hillock on KDP {101} at which no dislocations are observed. (b) Higher resolution 715 × 715 nm image of one such hillock showing the topmost island for which the radius is 42 nm.

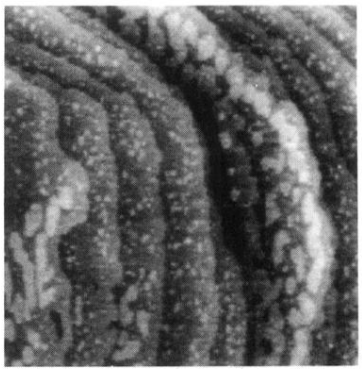

FIG. 4. 6.3×6.3 μm area near boundary between sectors 2 and 3 of hillock in Fig. 3(a). Note the presence of islands on all terraces.